

# Use of the electrocoagulation with pomegranate peels and zizith's leaves adsorption coupling technique for removal of methylene blue in a batch system

Raghda M. Alnawab<sup>1</sup>, Ali Mousa Ridha<sup>1\*</sup>

<sup>1</sup> Department of Materials Engineering Technology, Engineering Technical College–Baghdad, Middle Technical University, Baghdad, Iraq

\*Corresponding author E-mail:

## Abstract

The present work is concerned with the remediation MB of aqueous solution by exploring the batch electrocoagulation process EC, and coupling the EC with biosorption on to pomegranate EC/PP and ziziphus EC/ZL. Batch experiments were conducted to investigate the EC, EC/PP, and EC/ZL processing at different parameters, such as, current density, pH, contact time and initial dye concentrations, NaCl concentration, distance between electrodes and biosorbents dosages for PP and ZL. The highest removal efficiency of EC (93.47%) was obtained at a current density of 21.440 A/m<sup>2</sup>, initial dye concentration of 100 mg/l, pH of 7, the NaCl concentration of 1.5 g/l, time of 60 minutes, and inter electrode distance of 1 cm. The energy consumption of electrodes was evaluated at these operating conditions to be 1.9 KW.h/m<sup>3</sup>. The maximum removal efficiency of the coupling treatment process EC/PP of 96% under optimum operating conditions of EC was achieved at 1500 mg of pomegranate peels, 30 min treatment time, and 1.3 KW.h/m<sup>3</sup> of energy consumption of electrodes. From the comparison between EC, EC/PP, and EC/ZL techniques, it can be seen that the coupling technique EC/PP is the best method for removal of MB dye than EC and EC/ZL. The Langmuir isotherm fits the experimental data better than Freundlich and Temkin adsorption isotherm for the EC process alone, EC/PP and EC/ZL processes.

**Keywords:** Electrocoagulation; Methylene Blue (MB); Pomegranate Peels; Ziziphus Leaves; Adsorption.

## 1. Introduction

One of the main problems of the society in the 21 century is environmental pollution. The presence of chemically different dyes in the environment has been contributed as a major part of water pollution. Many industries are directly or indirectly discharged wastewater into the surface water with high levels of a variety of dyes [1].

Methylene blue dye is widely used in a number of industries such as textile, tannery, dye manufacturing, temporary air, pharmaceutical industries, and paper and pulp industries. The textile industry is one of these activities that produce large quantities of impure water and chemical products [2]. This contaminated substance is toxic and can lead to serious problems and threats to human health. Many of various dye effluents contain the chemical output, which are toxic, carcinogenic (can cause cancer) or mutagenic (can cause mutation) two forms of life, mainly due to carcinogens, such as Benzadrine, naphthalene and other aromatic compounds. Therefore, it is important to immediately dyeing wastewater before discharge into the water environment [3].

There are many methods to remove dyes from wastewater, the most common ones are coagulation and/or flocculation, precipitation, ion exchange, membrane technology, biological treatment, advanced oxidation treatment, adsorption and electrocoagulation techniques were used to treat organic pollutants such as dyes from contaminated water and wastewater [4-5] Most of these approaches are unsuitable and insufficient due to the dyeing wastewater contain large amount of aromatic compound structures. Adsorp-

tion has more advantages than other methods due to its simple design and it could include a low initial investment and the required land. The adsorption process is widely used to treat industrial wastewater from organic and inorganic pollutants and meet the great interest of researchers [6-7]. A simple and efficient sewage treatment process is essential. The electrical process of coagulation (electro-coagulation) is appears to be a reliable technology effective. Electrocoagulation (EC) is exceptionally successful in removing organic pollutants, including dyeing wastewater. Electro-coagulation is simple in operation and requires little space. The sludge produced during electro-coagulation process is less as compared to coagulation process [8].

The main objective of the current work is to use a clean and environmentally friendly approach to remove the of Blue dye methylene from aqueous solution by coupling electrocoagulation technique with adsorption. The effect of process parameters like current density, initial concentration of MB, time of electrolysis, the space between electrodes, pH and concentration of NaCl were studied. The efficiency of coupling the electrocoagulation process with adsorption onto pomegranate peel (EC/PP) and ziziphus leaves (EC/ZL) for remediation methylene blue dye from aqueous solution was evaluated and compared between them.

## 2. Material and methods

### 2.1. Materials

The methylene blue dye (MB)  $C_{16}H_{18}N_3SCl$ , that was used in this work as an adsorbate was supplied by CDH company, (India). Pomegranate peels were bought from the local market. Ziziphus leaves were collected from local gardens. The iron plates used in this study as electrodes were bought from local markets. The characteristics of the iron plate analyzed by state company for inspection and engineering rehabilitation (SIER) in Iraq to be as shown in Table 1.

**Table 1:** Analysis of Iron Electrode Properties

Composition	Wt. %
Fe	98.80
C	0.0994
Mn	0.6600
S	0.1900
Al	0.1030
Others	0.1447

## 2.2. Experimental

### 2.2.1. Preparation of MB Dye stock solution

Methylene blue, a cationic dye  $C_{16}H_{18}N_3SCl$  was used as a pollutant. A certain amount of NaCl was added into the MB solution as supporting electrolyte. By adding 1gm of methylen blue (MB) into 1L of distilled water prepare a stock solution of MB dye. The solution of MB with different initial concentration is prepared by diluting the solution of the stock. The calibration curve was constructed using a UV spectrophotometer (Model 6310, Jenway Company, England) at a maximum wavelength of 665nm. The concentrations of remaining MB dye solution were measured using UV-Visible spectrophotometer.

### 2.2.2. Design of electrocoagulation reactor

The batch electrocoagulation cell used in this work was made of perspex with dimensions of (120 mm x 120 mm x 180 mm). There are eight iron plate electrodes with the same dimensions that used as four anodes and four cathodes. The dimensions of electrodes were (80 mm x 70 mm x 1 mm) and the total effective surface area of anodes was 466.4 cm<sup>2</sup>. The total immersed area of each electrode was 116.6 cm<sup>2</sup>. In this work, the ratio of the effective immersed area to the volume of the solution was fixed at (466.4/2016) m<sup>2</sup>/m<sup>3</sup>. This ratio was designed based on the recommendations of (Brahmi, et al., 2014) [9].

### 2.2.3. Preparation of pomegranate and Ziziphus as an adsorbents

Fresh pomegranate and ziziphus were used. The peels were manually separated from core pomegranate. Then, the pomegranate peels and ziziphus leaves were washed extensively several times with distilled water to remove dust particles, impurities and any other stakes. They were chopped into small pieces and dried in an oven at 60°C for 48 h. The dried pieces were crushed, ground and sieved to obtain the desired particle size range (250-400) micrometer. After sieving, the resulted particles of each material were kept in a desiccator for further use in EC experiments.

### 2.2.4. Batch electrocoagulation technique (EC)

The Electrocoagulation (EC) experiments were performed in a batch mode using 1.5 liter rectangular cell. The iron electrodes (anodes and cathodes) were polished with abrasive emery paper, washed with diluted HCl and then rinsed several times with distilled water. The desired pH of the MB dye solution was adjusted using diluted 1M HCl or 1M of NaOH before each run of EC. Eight vertical electrodes (four anode and four cathode electrodes) were used with a distance between anodes and cathodes of 1 cm. The electrodes were electrically connected to the DC digital power supply (type PS-305D, Dazheng, china) and operated in monopolar mode.

A 1500 ml of MB dye solution at initial concentration 100 ppm was added into EC reactor and then stirred by a magnetic stirrer at stirring speed of 300 rpm and at 25°C. During stirring, a certain amount of sodium chloride was added to the solution to obtain the desired solution conductivity. The current density and initial pH of the solution were adjusted to known values. The samples were periodically withdrawn from an electrocoagulation cell at different time intervals. Then, solution sample was separated by filtration using a Millipore Membrane filter with pore size 0.45µm. The 665nm wavelength of ultraviolet-visible spectrophotometer was used to analyze the equilibrium concentrations of MB dye in the filtrate.

### 2.2.5. Treatment procedure of combining EC and adsorption process (second treatment)

Adsorption process was carried out in electrolytic cell using Pomegranate and ziziphus leaves as bioadsorbents. The best operating conditions of the EC process (current density, initial concentration of the MB dye solution, pH of MB solution, time, NaCl Dosage and distance between electrodes) were taken and then followed by the adsorption process (second treatment).

Different adsorbent dosage of (500, 750, 1000, 1500 and 2000) mg/l of pomegranate peels and (500, 750, 1000, 1500, 2000, 2500 and 3000) mg/l of ziziphus leaves were mixed with 1500 ml of MB dye solution at certain initial concentration prior to each run. MB dye solution at initial concentration 100 ppm was added into the EC rectangular reactor with eight electrodes (four anodes and four cathodes). The solution was then stirred by a magnetic stirrer to obtain homogeneous composition of the synthetic MB dye solution and bioadsorbents. The speed of the stirrer and the temperature are fixed at 300 RPM and 25°C respectively. The desired conductivity of the solution was obtained when adding specific amount of sodium chloride in 1500 ml of the MB dye solution. The current density and the initial pH of the solution were maintained to a known value. The samples were periodically withdrawn from an electrocoagulation cell at different time intervals. Then, solution sample was separated by filtration using a Millipore Membrane filter with pore size 0.45µm. The 665nm wavelength of ultraviolet-visible spectrophotometer was used to analyze the equilibrium concentrations of MB dye in the filtrate.

In this work, the range of operating parameters used to remove MB dye from synthetic solution is presented in Table 2. The best operating conditions of the EC process for maximum removal MB dye from synthetic solution were then selected.

**Table 2:** Parameters Studied in This Work

Parameters	
Current Density, A/m <sup>2</sup>	(0.43-42.9)
Initial Concentration, mg/l	(50-250)
pH	(2-10)
Time, min	(10-90)
Space between electrodes, cm	(1-3)
NaCl, g/l	(0.5-2)
Biosorbents dosage (PP and ZI), g/l	(0.5-3)

## 2.3. Power consumption

The power utilized by the reactor can be easily modeled as the product of the current and the used potential. In reality, the potential varies throughout galvanostatic reactor operation, so the parameters must be integrated over time. Electrical energy consumption and current efficiency are very important economical parameters in the EC process. Electrical energy consumption can be calculated by the following Eq. (1): [10]

$$E = (U * I * t_{EC}) / V \quad (1)$$

Where E is electrical energy in kWh (m<sup>3</sup>)<sup>-1</sup>. U is cell voltage in volt (V). I is applied current (A). V is volume of solution (m<sup>3</sup>). t<sub>EC</sub> is the electrolysis time per hour.

## 2.4. Adsorbents characterization

Pomegranate peels and ziziphus leaves have been characterized using Fourier transform infrared (FTIR) spectroscopy (Model IRTracer-100, Shimadzu Company, Japan). FTIR analysis was performed in the range of 400-4000  $\text{cm}^{-1}$  to identify the surface functional groups in the complex nature of adsorbent (pomegranate peels and ziziphus leaves). The EC by-product using iron electrode was characterized by X-ray diffraction to confirm the existence of the generated coagulant and Fourier transform infrared spectroscopy (FTIR) of the sludge after treatments of MB dye from synthetic solution.

### 2.5 Adsorption Isotherm

Adsorption isotherm is a curve related to the balance of dissolved concentration on the surface of the adsorbent material,  $q_e$ , to the dissolved concentration in the liquid,  $C_e$ , with which it is in contact. The adsorption isotherm is also a function of the solute amount adsorbed on the solid and the equilibrium concentration of the solute in solution at a certain temperature. It is important to study the equilibrium coefficient and adsorption capacity for adsorption through the analysis of the equilibrium adsorption isotherms data [11]. Adsorption is an important process that describes the interaction of adsorbents and dye ion to develop a design model for wastewater treatment.

Experimental adsorption capacities and dye concentration (adsorption isotherm) was applied extensively by the Langmuir, Freundlich and Temkin models. The amount of adsorption at equilibrium,  $q_e$  (mg/g), is given by Eq. 1 [12].

$$q_e = \frac{V}{m} (C_0 - C_e) \quad (2)$$

Where  $C_0$  and  $C_e$  (mg/l) are the initial and equilibrium concentration of adsorbate, respectively,  $V$  (l) is the volume of the solution, and  $m$  (g) is the adsorbent mass. According to the general formula (Eq. 2), the efficiency of sorption can be described by an adsorption isotherm [12].

$$\text{Sorption Efficiency, \%} = \frac{(C_0 - C_e)}{C_0} * 100 \quad (3)$$

There are several models for predicting the equilibrium distribution. However, the Langmuir Isotherm Temkin Isotherm and Freundlich Isotherm models are most commonly observed.

#### 2.4.1. Langmuir isotherm model

The Langmuir sorption isotherm model is probably the best and most widely applied sorption isotherm. This model quantitatively describes the formation of a single-layer adsorbate on the outer surface of the adsorbent, and then no further adsorption occurs. Langmuir therefore represents the equilibrium distribution of metal ions between the solid and liquid phases. Langmuir isotherm is represented in Eq. (3): [13-14]

$$q_e = \frac{q_m k_L C_e}{1 + k_L C_e} \quad (4)$$

The above equation can be rewritten in Eq. (4) [15]:

$$\frac{1}{q_e} = \frac{1}{q_m} + \frac{1}{q_m k_L C_e} \quad (5)$$

Where  $C_e$  is the equilibrium adsorbate concentration in the solution (mg/l).  $q_e$  is the equilibrium adsorbate concentration (mg/g) on the adsorbent.  $k_L$  is Langmuir constants (l/g).  $q_m$  is the maximum adsorption capacity (mg/g).

#### 2.4.2. Freundlich isotherm model

It is a curve associated with the solute concentration on the surface of an adsorbent, to the solute concentration in the liquid that is in contact with it. The Freundlich isotherm can be derived assuming

a logarithmic reduction in the enthalpy of adsorption with the increase in the fraction of occupied sites. The model and is usually presented by the following non-linear Eq (5) [14].

$$q_e = k_f C_e^{1/n} \quad (6)$$

The logarithmic form of the equation becomes:

$$\log q_e = \log k_f + \frac{1}{n} \log C_e \quad (7)$$

Where  $k_f$  is a constant describing the adsorption capacity (l/g) and  $n$  is an empirical parameter related to the adsorption intensity. The constants  $n$  and  $k_f$  were obtained from the slope and intercept respectively.

#### 2.4.3. Temkin isotherm model

This isotherm contained in a factor that is explicitly taking into account and intensified reactions. As is clear from the equation, the derivation is characterized by a uniform distribution of binding energies (up to some maximum binding energy) was carried out by plotting the quantity sorbed  $q_e$  vs.  $\ln C_e$ . The constants were determined from the slope and intercept, and the model is given by the following Eq. (7): [16]

$$q_e = \frac{RT}{b \ln(A_T C_e)} \quad (8)$$

$$q_e = \frac{RT}{b \ln A_T} + \left[ \frac{RT}{b} \right] \ln C_e \quad (9)$$

$$B = \frac{RT}{b} \quad (10)$$

$$q_e = B \ln A_T + B \ln C_e \quad (11)$$

Where  $B = [RT/bT]$  is corresponding to the heat of adsorption in (J/mol).  $R$  is the ideal gas constant (8.314J/mol.K).  $T$  (K) is the absolute temperature at 298K.  $A_T$  is the Temkin isotherm constant and  $A$  (l/g) is the equilibrium binding constant corresponding to the maximum binding energy [17].

## 3. Results and discussion

### 3.1. Characterization of the adsorbents

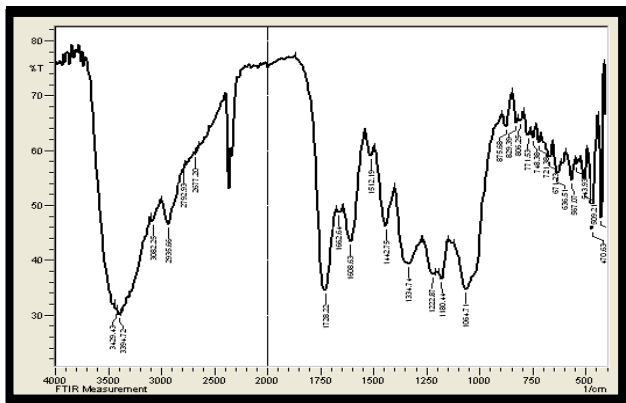
#### 3.1.1. FTIR

The Fourier transform infrared spectroscopy (FTIR) of the pomegranate peels before and after treatments of MB dye from synthetic solution are presented in Figures 1 and 2, respectively. The band, at around 3429  $\text{cm}^{-1}$ , can be attributed to hydroxide ions OH-1 group (carboxylic acid and phenolic). The band at around 2935  $\text{cm}^{-1}$  can be assigned to bond C-H stretching ( $-\text{CH}_3$  and  $\text{CH}_2$ ). The broadband presented at about 1748  $\text{cm}^{-1}$  ascribes to (C—C) stretching. The appearance of band at about 1662  $\text{cm}^{-1}$  is represented the aromatic group. While the band 1442  $\text{cm}^{-1}$  is characteristic of the bond (C-O) stretching vibrations. Stretching of alkane primary amine can be observed in the band (C-N) at about 1064  $\text{cm}^{-1}$ . These results are in agreement with the work of (Ahmad et al., 2014) [18]. The change in surface functional groups can be ascribed to the changes performed through adsorption process as shown in Figures 1 and 2. During the adsorption process, some functional groups were observed. Some of the groups were remained and the other groups were shifted.

FTIR of the ziziphus leaves before and after treatments of MB dye from synthetic solution are presented in Figures 3 and 4, respectively. FTIR spectrum after second treatment (EC/adsorption) shows that wave length and the intensity of some peaks are shifted or are substantially lower than those before adsorption. The band 3387  $\text{cm}^{-1}$  corresponding to O—H or N—H groups is shifted to 3417.86  $\text{cm}^{-1}$ . The peak 2931.80  $\text{cm}^{-1}$  is attributed to C—H stretch-

ing vibration of  $CH_2$ . The band at  $1732.08\text{ cm}^{-1}$  is ascribed to carbonyl C-O groups. The peak at  $1620.21\text{ cm}^{-1}$  may be attributed to C-O stretching vibration. The skeletal C-C vibrations in aromatic rings cause two bands at  $1516.06$ . The peaks at  $1442.75\text{ cm}^{-1}$ ,  $1369.46\text{ cm}^{-1}$ , and  $1319.31\text{ cm}^{-1}$  in the spectrum show C-N groups. Peaks in the range of  $1000\text{--}1200\text{ cm}^{-1}$  can be corresponded to C-O stretching. The relatively intense bands at  $1099.43\text{ cm}^{-1}$ ,  $1072.42\text{ cm}^{-1}$ ,  $1033.85\text{ cm}^{-1}$  can be assigned to alcohol groups (R-OH). The C-H out-of-plane bending in benzene derivative vibrations causes the band at  $837.11\text{ cm}^{-1}$ . The change in the surface functional groups can be ascribed to the changes performed through adsorption process as shown in Figures 3 and 4. During the adsorption process some functional groups observed, some remained and other shifted. The bands at  $3387\text{ cm}^{-1}$ ,  $2931.80\text{ cm}^{-1}$ ,  $1516.06\text{ cm}^{-1}$ ,  $1442.75\text{ cm}^{-1}$ ,  $1369.46\text{ cm}^{-1}$  and  $837.11\text{ cm}^{-1}$  are shifted to  $3417.86\text{ cm}^{-1}$ ,  $2920.23\text{ cm}^{-1}$ ,  $1558.48\text{ cm}^{-1}$ ,  $1438.90\text{ cm}^{-1}$ ,  $1327.03\text{ cm}^{-1}$  and  $829.39\text{ cm}^{-1}$  respectively [19].

The Fourier transform infrared spectroscopy (FTIR) of the iron sludge after treatments of MB dye from synthetic solution are presented in Figure 5. The presence of different functional groups in sludge sample shows electrolyte interaction between flocs. These cations play an important role for the removal of colloids during EC experiment [34]. Wavelength of carbonyl group lies between the regions of  $1083$  and  $1604\text{ cm}^{-1}$ . The bands in the region of  $1600\text{ cm}^{-1}$ ,  $447\text{ cm}^{-1}$  characterize the aromatic C=C stretching.



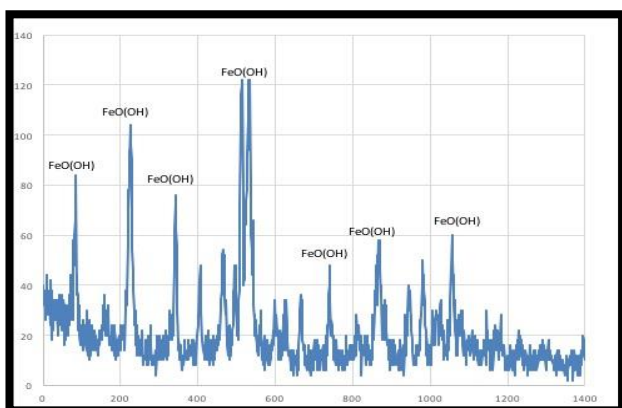


Fig. 6: XRD Analysis of the Sludge Generated During EC with Fe Electrodes.

### 3.2. Influence of current density

The results of these experiments are presented in Figure 7. It is evident that at all current densities (0.428-42.881 A/m<sup>2</sup>), the MB dye removal efficiency to be gradually increased from time 10-90 min. At current density of 0.428 A/m<sup>2</sup>, the MB dye removal efficiency was significantly affected (varied from 33 % to 63%) by the increase in the time. Whereas, at 1.286 A/m<sup>2</sup> and upward, the MB dye removal efficiency were significantly increased with increasing the time. This is due to the high cationic amount (Fe<sup>3+</sup>) of sacrificial electrode dissolution and (OH<sup>-</sup>) that generated into the MB dye solution and the faster MB dye concentration decreased. It is clearly attributed to reach equilibrium state between the generated coagulant (Fe(OH)<sub>n</sub>) and MB dye (pollutant). These results confirm the results of Sengil et al, (2009) [22].

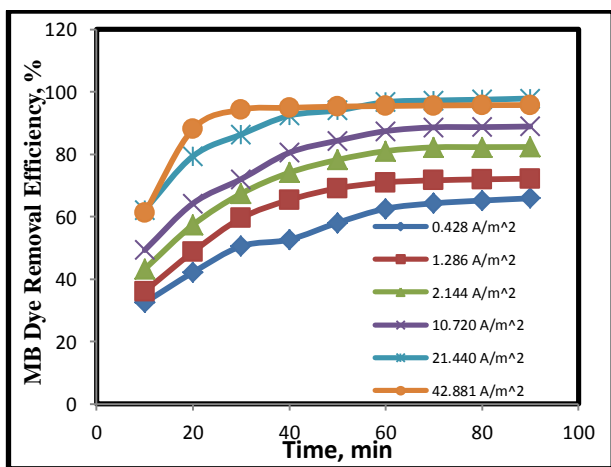


Fig. 7: Effect of Current Density.

Table 3 shows that the increase of the currents from 0.428 A/m<sup>2</sup> to 42.881 A/m<sup>2</sup> leads to a proportional increase of energy consumption from 0.01 Kw.h.m<sup>3</sup> to 9.4 Kw.h.m<sup>3</sup>. These results are in agreement with the work of (Merzouk et al., 2009) [23].

Table 3: The Energy Consumption and Current Density for MB Dye Removal from Aqueous Solution

Current Density, A/m <sup>2</sup>	Energy Consumption, Kw.h/m <sup>3</sup>
0.428	0.01
1.286	0.048
2.144	0.22
10.72	0.8
21.44	1.9
45.88	9.4

### 3.3. Influence of MB Dye initial concentration

Figure 8 shows the results of these experiments at (best current density =21.440 A/m<sup>2</sup>, pH=7, NaCl= 1g/l, Time= 90 mins and D<sub>c</sub>=1 cm). It can be seen that the increasing of initial MB dye

concentration decreases the efficiency of MB dye removal. The maximum efficiencies of MB dye removal at the initial MB dye concentrations (150, 200 and 250) ppm varied (from 41 % to 85 %), (from 22 % to 77 %) and (from 20 % to 71 %) respectively. This results are similar to the results of Golder et al, (2006) [38]. All cationic amounts Fe<sup>3+</sup> from sacrificial elect. rod (anode) were released into MB dye synthetic solution in the EC cell. This leading to formation of polymeric species and precipitated Fe (OH)<sub>3</sub> (as coagulant) as a result, it enhanced the MB dye remediation from synthetic solution.

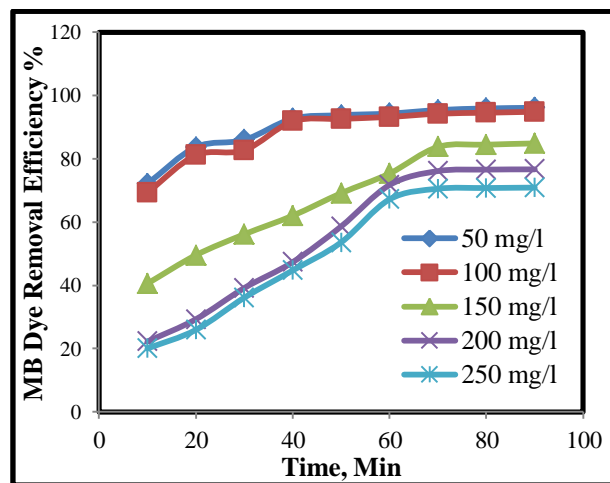


Fig. 8: Effect of Initial Dye Concentration.

Table 4 shows that increasing of the MB initial concentration from 50 mg/l to 250 mg/l leads to proportional increase of energy consumption from 1.7 Kw.h/m<sup>3</sup> to 4.1 Kw.h/m<sup>3</sup> after 90 min.

Table 4: The Energy Consumption and Initial Dye Concentration Necessary to Remove MB Dye from Aqueous Solution

Initial Dye Concentration mg/l	Energy Consumption Kw.h/m <sup>3</sup>
50	1.7
100	1.9
150	3.0
200	3.6
250	4.1

### 3.4. Influence of pH

From the results, shown in Figure 9, it can be seen that the efficiency removal of MB dye started gradually increased from 68% to 94 % with increasing from pH 2 to 6. Where at pH > 6, the efficiency removal significantly decreased with increasing of pH. This decrease in the MB dye removal efficiency in acidic and alkaline medium is caused by an amphoteric behavior of iron species which led to soluble monomeric hydrolysis species (Fe<sup>3+</sup>) at acidic pH and Fe(OH)<sub>4</sub><sup>-</sup> at alkaline medium. These soluble coagulants have insignificant effects on the MB dye removal efficiency from aqueous solution. For pH around neutrality (between 6 and 7), iron hydroxide insoluble coagulants are the primary species, with very few amounts of soluble species which lead to a more effective treatment. Therefore, the pH of 6 was selected as the optimum pH of MB solution in order to obtain maximum removal efficiency.

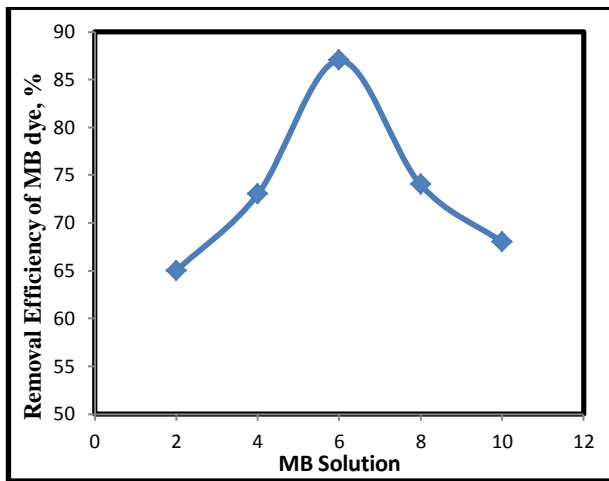


Fig. 9: Effect of pH.

### 3.5. Influence of sodium chloride concentration

The results of NaCl concentration effect on MB dye removal was as shown in Figure 10. It is observed that MB dye removal efficiency started to increase gradually with increasing the NaCl concentrations due to the increase in solution conductivity. The maximum removal efficiency of MB dye 94% were presented at higher concentrations of sodium chloride 1, 1.5, and 2 g/l and beyond 70 min, respectively. While no significant affect in MB removal efficiency with 0.5 g/l of NaCl concentration is observed. This behavior can be attributed to the ability of chloride ions to destroy the oxidation layer that formed on the electrodes surfaces. This leads to improve the dissolution rate of anode electrodes and increase the creation of coagulants that act as adsorbent in bulk solution. These results are agreement with the work of (Golder et al., 2010) [24].

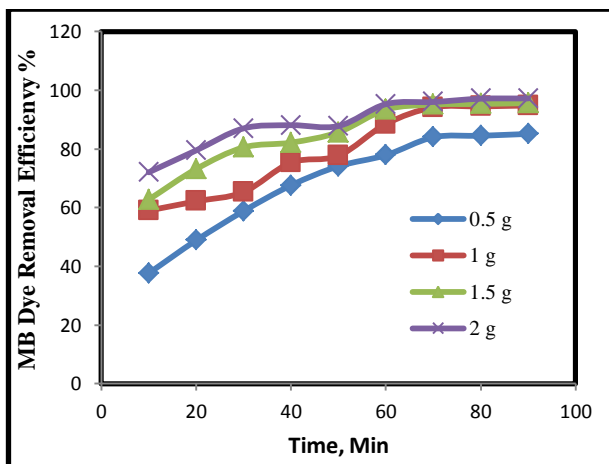


Fig. 10: Effect of Sodium Chloride Concentration.

### 3.6. Influence of inter electrode distance

Figure 11 shows the experimental results for the effect of inter electrode distance on the MB dye removal efficiency. It can be seen from the results, that the MB dye removal efficiency decreased with increasing inter electrodes spacing, electrical resistance between electrodes was increased and current passed through electrodes was decreased. The decreasing of current, lead to lower production of hydroxyl ions. Hence, the dye removal efficiency was decreased, agree with the work of (Dabrowski et al., 2001) [25]. When the inter electrode spacing is increased less attraction by electrodes is applied on generated iron polymers. Their movement would be slower, and they tend to aggregate in flocs, and therefore enhancing dye molecules adsorption. When the distance is more than 1 cm dye molecule and flocs interactions are weaker leading to the decrease of the removal efficiency. Best

efficiencies are obtained with short distance, confirm with the results of (Khattari et al., 1999) [26]. The maximum removal efficiency of 94.9% was found at 10 mm distance, whereas at 30 mm distance, the removal efficiency was significantly decreased to 81.7% as showed in Figure 11.

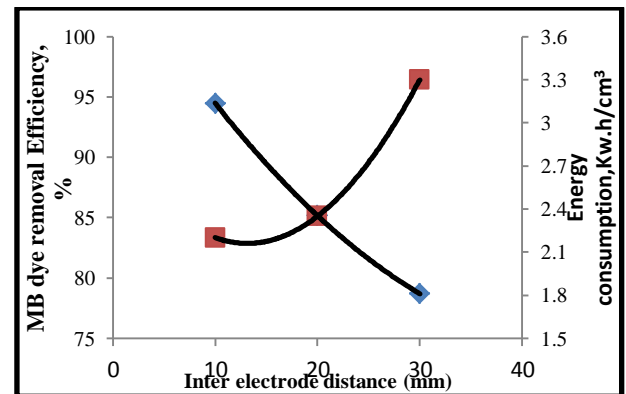


Fig. 11: The Effect of Inter Electrodes Distance.

### 3.7. Influence of pomegranate peels dosage

Figure 12 shows the effect of the dosage of pomegranate peels on the MB dye removal efficiency. From the obtained results at all dosages of pomegranate peels, it can be seen that the MB dye removal efficiency to be gradually increased in the period between 10-90 min. The MB removal efficiency from synthetic solution at 500, 750 mg of PP dosage increased gradually to reach its maximum after 50min, while in the adsorbents dosages (1000, 1500, 2000mg), the removal efficiency sharply increased to reach at 40min. It is clear that, when the dosage changed from low (500mg and 750 mg) of PP, the initial MB removal efficiency varied from 47.5% to 93%) and from 60% to 94.7% by increasing of the time respectively. Whereas adding high dosage at 1000mg, 1500mg and 2000 mg of PP, the MB dye removal efficiency were significantly increased (from 62% to 97%), (from 76.4% to 97.6%), (from 80% to 99%) respectively. A further increase in all adsorbents dosage after 40min showed no significant affect on the removal efficiency. This can be due to the fact that the solution was reached equilibrium between the adsorbent and adsorbate. This behavior can be explained by increasing the available number of adsorption surface sites, which results in an increase in removal efficiency of the MB dye in all adsorbents with increasing adsorbent dose which agrees with (Alsawalha, 2012) [27].

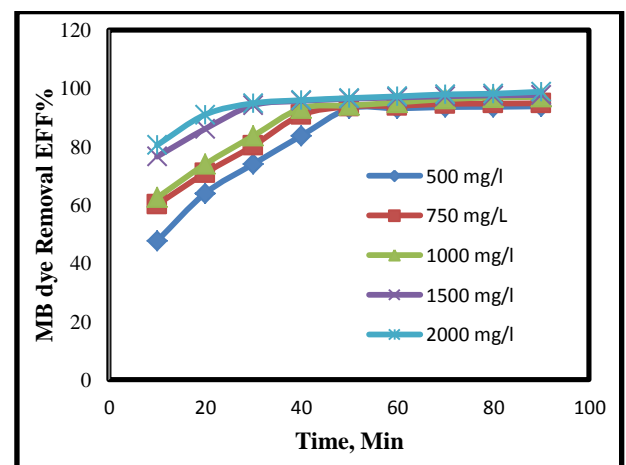


Fig. 12: The Effect of Pomegranate.

### 3.8. Influence of ziziphus leaves dosage

Figure 13 shows the effect of ziziphus leaves dosages on MB dye removal efficiency. It is clearly that at all dosage of ziziphus leaves, the MB dye removal efficiency were gradually increased in the

period of time 10-90 min. The MB removal efficiency from synthetic solution at 500, 1000 and 2000 mg of ZL dosage increased gradually up to 60 min, while in the adsorbents dosages (2500 and 3000 mg), the removal efficiency greatly increased up to 50min. At dosages 500 mg/L, 1000 mg/L of ziziphus leaves coupling with EC process, the MB dye removal efficiency was increased (from 38 % to 93 %), and from (48 % to 93 %) respectively with the time. But at 2000 mg and 2500mg dosages of ziziphus leaves, the MB removal efficiency was increased by the coupling treatment process (from 59 % to 94 %), and (from 63 % to 94 %) respectively. In addition, at 3000 mg of ziziphus leaves dosages the efficiencies were varied (from 66 % to 96 %). This reveals that the dye removal increases with the increase in adsorbent dosage. These results agree with work of (P. Sharma et al, 2010) [28]. Also, after that the adsorption efficiency remains constant and increased slowly even with the increase of ZL dosage due to the shortage of MB dye concentration in the solution. Thus, the initial MB dye concentration was kept constant for all varying dosage. This indicates that the rate of free ions ( $Fe^{+3}$ ) becomes constant with the increase in the adsorbent dose. These results agree with (Finotelli et al, 2008) [29].

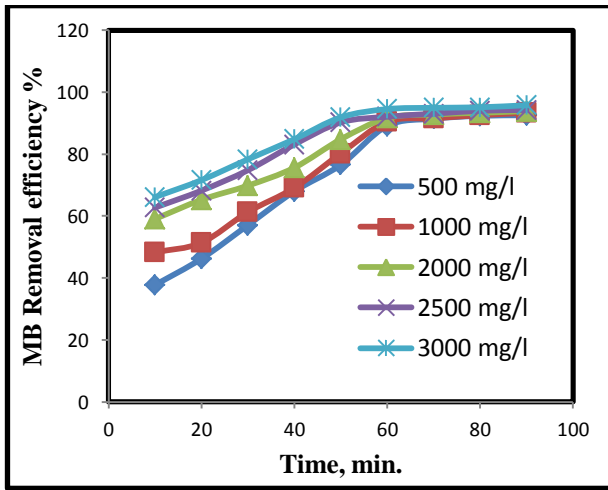


Fig. 13: Effect of Ziziphus Dosages.

### 3.9. Treatment appearance

Figure 14 shows the visible arrangement of MB dye in the treated solution with batch EC cell. The best operating conditions of EC process current density 21.440 A/m<sup>2</sup>, initial concentration of MB dye solution 100 mg/l, pH of MB solution at 7, time 90 min, NaCl Dosage at 1.5 g/l and distance between electrodes 1 cm were applied and then followed by adsorption process (second treatment). These samples were taken at 10, 20, 30, 40, 50, 60, 70, 80, 90 min from right to left respectively. This observation clearly indicates that the color decreases slightly with increasing treatment time.

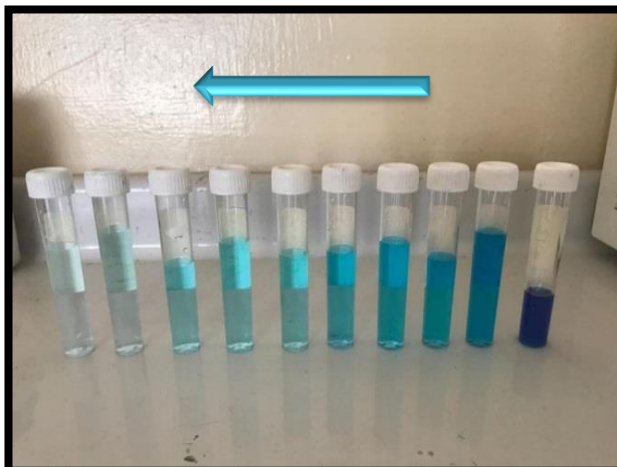


Fig. 14: Samples Taken at Each 10 Minutes of EC.

### 3.10. Adsorption isotherms

The experimental data for MB dye removal by EC process, EC/PP process and EC/ZL process are correlated with the three theoretical adsorption isotherm models. Figures 15, 16 and 17 show the adsorption isotherm curves for MB dye removal using EC process, EC/PP process and EC/ZL process. These Figures describe the experimental data and the theoretical data obtained from Langmuir, Freundlich and Temkin isotherm. All constants and correlation coefficients for Langmuir, Freundlich and Temkin isotherm theoretical model are listed in Table 5. Based on the correlation coefficient ( $R^2$ ) for the EC, and the coupling processes (EC/PP), and (EC/ZL) listed in Table 4.8 for various models, it can be concluded that Langmuir isotherm give a better model description to the experimental data than Freundlich and Temkin isotherm for MB removal from synthetic solution.

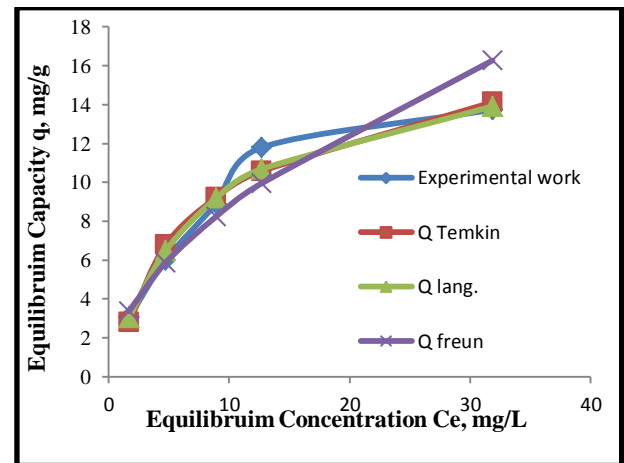


Fig. 15: Adsorption Isotherms of EC Process.

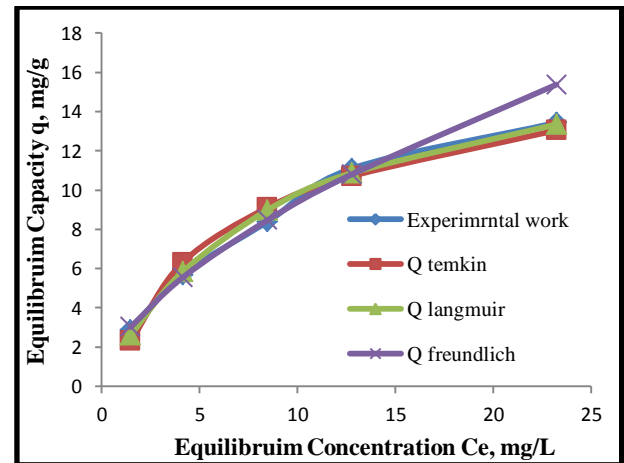


Fig. 16: Adsorption Isotherms of EC /PP Process.

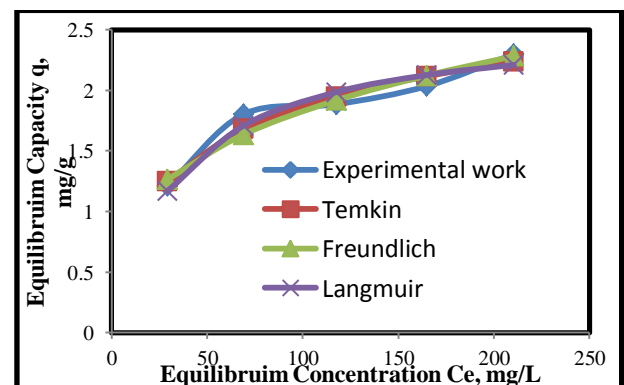


Fig. 17: Adsorption Isotherms of EC /ZL Process.

**Table 5:** Langmuir, Freundlich and Temkin Isotherm Constants for the MB Removal by EC Process, EC/PP Process and EC/ZL Process

Theoretical Models	Adsorbents			
	EC	EC/PP	EC/ZL	
Langmuir Isotherm	$q_m$	17.3913	18.5185	2.5793
	$K_L$	0.1252	0.1110	0.0283
	$R^2$	0.9906	0.9918	0.9873
	$n$	1.87	1.69	3.35
Freundlich Isotherm	$K_f$	2.5527	2.3905	0.4616
	$R^2$	0.949	0.9695	0.9428
	$A_T$	1.2262	1.2151	0.4192
	$b_T$	643.1409	634.4777	4962.091
Temkin Isotherm	$B$	3.8523	3.9049	0.4993
	$R^2$	0.9678	0.9781	0.9530

## 4. Conclusions

This work aimed to investigate the remediation of Methylene Blue dye (MB) from aqueous solution by eco-friendly approaches, an electrocoagulation technique (EC) and coupling of an electrocoagulation treatment with pomegranate peels (PP) and ziziphus leaves (ZL) adsorption process. For batch electrocoagulation technique (EC), the maximum removal efficiency of MB dye is 93.47% obtained at optimal conditions. The optimal operating conditions namely current density 21.440 A/m<sup>2</sup>, initial concentration of MB dye solution 100 mg/l, pH of MB solution at 7, time 60 min, NaCl dosage at 1.5 g/l and distance between electrodes 1 cm are obtained in this work.

Natural agricultural wastes namely pomegranate peels (PP) and Ziziphus leaves (ZL) have been utilized to remove the MB dye from aqueous solution. The addition of PP and ZL as bioadsorbents to an electrocoagulation process exhibited an improvement in MB dye removal efficiency.

## References

- U. D. Gul and G. Donmez, Effect of A Cationic Surfactant on Dye Biosorption Properties of Aspergillus Versicolor. Ommun. Faculty Science University Ankara Series C, 22 (2010) 1-13.
- K. Tanzim and M. Z. Abedin, Adsorption of Methylene Blue from Aqueous Solution by Pomelo (Citrus Maxima) Peel. International Journal of Scientific & Technology Research, 4 (2015) 2277-8616.
- R. Kant, Textile Dyeing Industry an Environmental Hazard. Natural science Journal, 4, 1 (2012) 22-26.
- A. Gurses, M. Yalcin and C. Dogar, Electrocoagulation of Some Reactive Dyes: A Statistical Investigation of Some Electrochemical Variables. Waste Management Journal, 22 (2002) 491-499. [https://doi.org/10.1016/S0956-053X\(02\)00015-6](https://doi.org/10.1016/S0956-053X(02)00015-6).
- E. Forgacs, T. Cserhati and G. Oros, Removal of Synthetic Dyes from Wastewaters: A Review. Environment International Journal, 30 (2004) 953-971. <https://doi.org/10.1016/j.envint.2004.02.001>.
- D. Ghosh and K. G. Bhattacharyya, Adsorption of Methylene Blue on Kaolinite. Applied Clay Science, 20, (2002) 295-300. [https://doi.org/10.1016/S0169-1317\(01\)00081-3](https://doi.org/10.1016/S0169-1317(01)00081-3).
- C. Namasivayam and D. Kavitha, Removal of Congo red from Water by Adsorption Onto Activated Carbon Prepared from Coir Pith, An Agricultural Solid Waste. Dyes and Pigments, 54 (2002) 47-58. [https://doi.org/10.1016/S0143-7208\(02\)00025-6](https://doi.org/10.1016/S0143-7208(02)00025-6).
- D. O. Siringi, P. Home, J. S. Chacha and E. Koehn, Is Electrocoagulation (EC) A Solution to The Treatment of Wastewater and Providing Clean Water for Daily Use. ARPN Journal of Engineering and Applied Sciences, 7 (2012) 1819-6608.
- B. Khaled, B. Wided, H. Bechir, A. Limam, L. Mouna and Z. Tlili, Investigation of Electrocoagulation Reactor Design Parameters Effect on the Removal of Cadmium from Synthetic and Phosphate Industrial Wastewater. Arabian Journal of Chemistry, 14 (2014) 1-40.
- M. C. Hernandez, L. Barletta, M. B. Dogliotti, N. Russo, D. Fino and P. Spinelli, Heavy Metal Removal by Means of Electrocoagulation Using Aluminum Electrodes for Drinking Water Purification. J Appl Electrochem, 42 (2012) 809-817. <https://doi.org/10.1007/s10800-012-0455-8>.
- A. H. Sulaymon, T. J. Mohammed and J. Al-Najar, Equilibrium and Kinetics Studies of Adsorption of Heavy Metals onto Activated Carbon. Canadian Journal on Chemical Engineering & Technology, 3, 4, (2012) 86-92.
- M. Sarioglu and U. A. Atay, Removal of Mythelen Blue by Using Biosolid. Global NEST Journal, 8, 2 (2006) 113-120.
- E. Butler, Y. Hung, R. Y. Yeh and M. S. Al Ahmad, Electrocoagulation in Wastewater Treatment, Water Journal, 3 (2011) 495-525. <https://doi.org/10.3390/w3020495>.
- M. H. Abdul Latif, T. H. Al-Noor and K. A. Sadiq, Adsorption Study of Symmetrical Schiff Base Ligand 4, 4'- [hydrazine-1, 2-diylidenebis (methan-1-yl-1-ylidene) bis (2- methoxyphenol)] on Granulated Initiated Calcined Iraqi Montmorillonite via Columnar Method. Advances in Physics Theories and Applications, 24 (2013) 38-51.
- N. Saibaba and P. King, Equilibrium and Thermodynamic Studies for Dye Removal Using Biosorption. International Journal of Research in Engineering & Technology, 1 (2013) 17-24.
- K. L. Dubrawski, Reactor Design Parameters, In-Situ Speciation Identification, and Potential Balance Modeling for Natural Organic Matter Removal by Electrocoagulation. (2013) 1-195.
- M. R. Samarghandi, M. Hadi, S. Moayedi and F. B. Askari, Two-Parameters ISOTHERMS of Methyl Orange Sorption by Pinecone Derived Activated Carbon. Iran. Journal Environment Health Science Engineering, 6 (2009) 285-294.
- M. A. Ahmad, N. A. A. Puad and O. S. Bello, Kinetic, Equilibrium and Thermodynamic Studies of Synthetic Dye Removal Using Pomegranate Peel Activated Carbon Prepared by Microwave-Induced KOH Activation. Water Resources and Industry, 6 (2014) 18-35. <https://doi.org/10.1016/j.wri.2014.06.002>.
- A. Omri and M. Benzina, Removal of Manganese (II) Ions from Aqueous Solutions by Adsorption on Activated Carbon Derived a New Precursor: Ziziphus Spina-Christi Seeds. Alexandria Engineering Journal, 51 (2015) 343-350. <https://doi.org/10.1016/j.aej.2012.06.003>.
- M. Grube, J. G. Lin, P. H. Lee and S. Kokorevicha, Evaluation of Sewage Sludge-Based Compost by FT-IR Spectroscopy. Geoderma Journal, 130 (2006) 324-333. <https://doi.org/10.1016/j.geoderma.2005.02.005>.
- F. Ahangaran, A. Hassanzadeh and S. Nouri, Surface modification of Fe<sub>3</sub>O<sub>4</sub>@SiO<sub>2</sub> microspheres by silane coupling agent. International Nano Letters a springer Journal, 3 (2013) 1-5.
- I. A. Sengil and M. t Ozacar, the Decolorization of C.I. Reactive Black 5 in Aqueous Solution by Electrocoagulation Using Sacrificial Iron Electrodes. Journal of Hazardous Materials, 161 (2009) 1369-1376. <https://doi.org/10.1016/j.jhazmat.2008.04.100>.
- B. Merzouk, B. Gourich, A. Sekki, K. Madani, Ch. Vial and M. Barkaoui, Studies on the Decolorization of Textile Dye Wastewater by Continuous Electrocoagulation Process. Chemical Engineering Journal, 149 (2009) 207-214. <https://doi.org/10.1016/j.cej.2008.10.018>.
- A. K. Golder, H. Kumar, A. N. Samanta and S. Ray, Colour Diminution and COD Reduction in Treatment of Coloured Effluent by Electrocoagulation. International Journal Environmental Engineering, 2 (2010) 1-3.
- N. Daneshvar, H. A. Sorkhabi and A. Tizpar, Decolorization of Orange II by Electrocoagulation Method. Separation and Purification Technology, 31 (2003) 153-162. <https://doi.org/10.1016/j.cej.2008.10.018>.
- S. Aoudj, A. Khelifa, N. Drouichea, M. Hecini and H. Hamitouche, Electrocoagulation Process Applied to Wastewater Containing Dyes from Textile Industry. Chemical Engineering and Processing: Process Intensification, 49 (2010) 1176-1182. <https://doi.org/10.1016/j.cep.2010.08.019>.
- M. Alsawalha, Instrumental Characterization of Clay by FTIR, XRF, BET and, TPD-NH<sub>3</sub>. International Conference on Agriculture, Chemical and Environmental Sciences, (2012) 125-128.
- P. Sharma, R. Kaur, C. Baskar and W. J. Chung, Removal of Methylene Blue from Aqueous Waste Using Rice Husk and Rice Husk Ash. Desalination, 259 (2010) 249-257. <https://doi.org/10.1016/j.desal.2010.03.044>.
- P. V. Finotelli, D. A. Sampaio, M. A. Morales, A. M. Rossi and M. H. R. Leao, Ca Alginate as Scaffold for Iron Oxide Nanoparticles Synthesis. Brazilian Journal of Chemical Engineering, 25, 4 (2008), 759-764. <https://doi.org/10.1590/S0104-66322008000400013>.
- S. Vasudevan J. Lakshmi and G. Sozhan, Studies on the Al-Zn-In-Alloy as Anode Material for the Removal of Chromium from Drinking Water in Electrocoagulation Process. Desalination, Vol. 275, (2011), pp. 260-268. <https://doi.org/10.1016/j.desal.2011.03.011>.